Photoproduction of the ρ^0 meson on the proton at large momentum transfer

M. Battaglieri,[1] E. Anciant,[2] M. Anghinolfi,[1] R. De Vita,[1] E. Golovach,[3] J.M. Laget,[2] V. Mokeev,[3] M. Ripani,[1] G. Adams,[26] M.J. Amaryan,[35] D.S. Armstrong,[34] B. Asavapibhop,[20] G. Asryan,[35] G. Audit,[2] T. Auger,[2] H. Avakian,[15] S. Barrow,[11] K. Beard,[16] M. Bektasoglu,[24] B.L. Berman,[12] N. Bianchi,[15] A.S. Biselli,[26] S. Boiarinov,[14] D. Branford,[19] W.J. Briscoe,[12] W.K. Brooks,[31] V.D. Burkert,[31] J.R. Calarco,[21] G.P. Capitani,[15] D.S. Carman,[23] B. Carnahan,[6] A. Cazes,[29] C. Cetina,[12] P.L. Cole,[30, 31] A. Coleman,[34] D. Cords,[31] P. Corvisiero,[1] D. Crabb,[33] H. Crannell,[6] J.P. Cummings,[26] E. DeSanctis,[15] P.V. Degtyarenko,[14] R. Demirchyan,[35] H. Denizli,[25] L. Dennis,[11] K.V. Dharmawardane,[24] K.S. Dhuga,[12] C. Djalali,[29] G.E. Dodge,[24] D. Doughty,[7] P. Dragovitsch,[11] M. Dugger,[4] S. Dytman,[25] M. Eckhause,[34] H. Egiyan,[34] K.S. Egiyan,[35] L. Elouadrhiri,[7] L. Farhi,[2] R.J. Feuerbach,[5] J. Ficenec,[32] T.A. Forest,[24] A.P. Freyberger,[31] V. Frolov,[26] H. Funsten,[34] S.J. Gaff,[9] M. Gai,[8] S. Gilad,[18] G.P. Gilfoyle,[28] K.L. Giovanetti,[16] K. Griffioen,[34] M. Guidal,[13] M. Guillo,[29] V. Gyurjyan,[31] D. Hancock,[34] J. Hardie,[7] D. Heddle,[7] F.W. Hersman,[21] K. Hicks,[23] R.S. Hicks,[20] M. Holtrop,[21] C.E. Hyde-Wright,[24] M.M. Ito,[31] K. Joo,[33] J.H. Kelley,[9] M. Khandaker,[22] W. Kim,[17] A. Klein,[24] F.J. Klein,[31] M. Klusman,[26] M. Kossov,[14] L.H. Kramer,[10, 31] Y. Kuang,[34] S.E. Kuhn,[24] D. Lawrence,[20] M. Lucas,[29] K. Lukashin,[31] R.W. Major,[28] J.J. Manak,[31] C. Marchand,[2] S. McAleer,[11] J. McCarthy,[33] J.W.C. McNabb,[5] B.A. Mecking,[31] M.D. Mestayer,[31] C.A. Meyer,[5] K. Mikhailov,[14] R. Minehart,[33] M. Mirazita,[15] R. Miskimen,[20] V. Muccifora,[15] J. Mueller,[25] G.S. Mutchler,[27] J. Napolitano,[26] S.O. Nelson,[9] B.B. Niczyporuk,[31] R.A. Niyazov,[24] J.T. O'Brien,[6] A.K. Opper,[23] G. Peterson,[20] S.A. Philips,[12] N. Pivnyuk,[14] D. Pocanic,[33] O. Pogorelko,[14] E. Polli,[15] B.M. Preedom,[29] J.W. Price,[26] D. Protopopescu,[21] L.M. Qin,[24] B.A. Raue,[10, 31] A.R. Reolon,[15] G. Riccardi,[11] G. Ricco,[1] B.G. Ritchie,[4] F. Ronchetti,[15] P. Rossi,[15] D. Rowntree,[18] P.D. Rubin,[28] K. Sabourov,[9] C. Salgado,[22] M. Sanzone-Arenhovel,[1] V. Sapunenko,[1] R.A. Schumacher,[5] V.S. Serov,[14] A. Shafi,[12] Y.G. Sharabian,[35] J. Shaw,[20] A.V. Skabelin,[18] E.S. Smith,[31] T. Smith,[21] L.C. Smith,[33] D.I. Sober,[6] M. Spraker,[9] A. Stavinsky,[14] S. Stepanyan,[35] P. Stoler,[26] M. Taiuti,[1] S. Taylor,[27] D.J. Tedeschi,[29] L. Todor,[5] R. Thompson,[25] M.F. Vineyard,[28] A.V. Vlassov,[14] L.B. Weinstein,[24] A. Weisberg,[23] H. Weller,[9] D.P. Weygand,[31] C.S. Whisnant,[29] E. Wolin,[31] M. Wood,[29] A. Yegneswaran,[31] J. Yun,[24] B. Zhang,[18] J. Zhao,[18] Z. Zhou,[18]

(CLAS Collaboration)

[1] *Istituto Nazionale di Fisica Nucleare, Sezione di Genova and Dipartimento di Fisica, Università di Genova, Italy 16146*

[2] *CEA-Saclay, Service de Physique Nucleaire, Gif-sur-Yvette, France 91191*

[3] *Moscow State University,Moscow, Russia 119899*

[4] *Arizona State University, Tempe, Arizona 85287-1504*

[5] *Carnegie Mellon University, Pittsburgh, Pennslyvania 15213*

[6] *Catholic University of America, Washington, D.C. 20064*

[7] *Christopher Newport University, Newport News, Virginia 23606*

[8] *University of Connecticut, Storrs, Connecticut 06269*

[9] *Duke University, Durham, North Carolina 27708-0305*

[10] *Florida International University, Miami, Florida 33199*

[11] *Florida State University, Tallahasee, Florida 32306*

[12] *The George Washington University, Washington, DC 20052*

[13] *Institut de Physique Nucleaire d'Orsay, IN2P3, BP 1, Orsay, France 91406*

[14] *Institute of Theoretical and Experimental Physics, Moscow, 117259, Russia*

[15] *Istituto Nazionale di Fisica Nucleare, Laboratori Nazionali di Frascati, Frascati, Italy 00044*

[16] *James Madison University, Harrisonburg, Virginia 22807*

[17] *Kyungpook National University, Taegu 702-701, South Korea*

[18] *Massachusetts Institute of Technology, Cambridge, Massachusetts 02139-4307*

[19] *University of Edinburgh, Edinburgh, Scotland, UK EH9 3JZ*

[20] *University of Massachusetts, Amherst, Massachusetts 01003*

[21] *University of New Hampshire, Durham, New Hampshirs 03824-3568*

[22] *Norfolk State University, Norfolk, Virginia 23504*

[23] *Ohio University, Athens, Ohio 45701*

[24] *Old Dominion University, Norfolk, Virginia 23529*

[25] *University of Pittsburgh, Pittsburgh, Pennslyvania 15260*

[26] *Rensselaer Polytechnic Institute, Troy, New York 12180-3590*

[27] *Rice University, Houston, Texas 77005-1892*

[28] *University of Richmond, Richmond, Virginia 23173*

[29] *University of South Carolina, Columbia, South Carolina 29208*

[30] *University of Texas at El Paso, El Paso, Texas 79968*

[31] *Thomas Jefferson National Accelerator Laboratory, Newport News, Virginia 23606*

[32] *Virginia Polytechnic Institute and State University, Blacksburg, Virginia 24061-0435*

The differential cross section, $d\sigma/dt$, for ρ^0 meson photoproduction on the proton above the resonance region ($2.6 < W < 2.9$ GeV) was measured up to a momentum transfer $-t = 5$ GeV^2 using the CLAS detector at the Thomas Jefferson National Accelerator Facility. The ρ^0 channel was extracted from the measured two charged-pion cross section by fitting the $\pi^+\pi^-$ and $p\pi^+$ invariant masses. The low momentum transfer region shows the typical diffractive pattern expected from Reggeon-exchange. The flatter behavior at large $-t$ cannot be explained solely in terms of QCD-inspired two-gluon exchange models. The data indicate that other processes, like quark interchange, are important to fully describe ρ photoproduction.

PACS : 13.60.Le , 12.40.Nn, 13.40.Gp

We report the results of ρ^0 meson photoproduction on protons for E_γ between 3.19 and 3.91 GeV. Data have been measured over the $-t$ range from $0.1-5.0$ GeV^2 using the CEBAF Large Acceptance Spectrometer (CLAS) at the Thomas Jefferson National Accelerator Facility (TJNAF). The low momentum transfer region ($-t < 1$ GeV^2), already measured in previous experiments [1,2] at similar energies, shows a diffractive behavior interpreted in the framework of the Vector Meson Dominance (VMD) model [3] as the elastic scattering of vector mesons off the proton target. In a more recent approach, this process is also described by the t-channel exchange of the Pomeron, scalar σ meson [4,5], and $f_2(1270)$ Regge trajectories [6].

At high $-t$, where the cross section is sensitive to the microscopic details of the interaction, the underlying physics can be described using parton degrees of freedom. In a QCD-inspired framework, the small impact parameter ($\approx 1/\sqrt{-t}$) prevents the constituent gluons (quarks) of the exchange from interacting and forming a Pomeron (Reggeon). Within certain models [7,8] this means that the constituents can be resolved into two-gluon (two-quark) structures (Fig. 1-a). Moreover, small transverse sizes select configurations where each gluon couples to different quarks both in the vector meson [8] and the nucleon [9], giving access to the correlation function in the proton (Fig. 1-b) [6]. The recent CLAS measurement of the ϕ photoproduction cross section [10], where the quark exchange is strongly suppressed by the OZI rule, was able to isolate the contribution due to two-gluon exchange. In the ρ case, its light quark composition also allows valence quarks to be exchanged between the baryon and the meson states (Fig. 1-c) [6].

A bremsstrahlung photon beam was produced by an $E_0 = 4.1$ GeV continuous electron beam hitting a gold radiator of 10^{-4} radiation lengths. The Hall B tagging system [11], with a photon energy resolution of 0.1% E_0, was used to tag photons in the energy range from $3.19-3.91$ GeV. The target cell, a mylar cylinder 6 cm in diameter and 18 cm long, was filled with liquid hydrogen at 20.4 K. During data taking at high intensity ($\sim 4\cdot 10^6\gamma$/s), the photon flux was continuously measured by an e^+e^- pair spectrometer located beyond the target. The efficiency of this device was determined during dedicated low intensity ($\sim 10^5\gamma$/s) runs by comparison with a 100% efficient lead-glass total absorption counter. The systematic uncertainty on the photon flux has been estimated to be 3% [10].

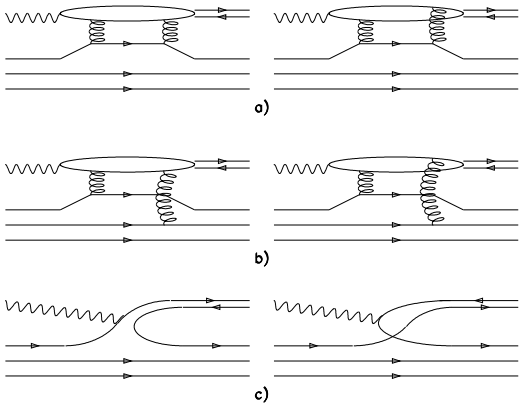

FIG. 1. The Feynman diagrams corresponding to a) two-gluon exchange from a single quark, b) two-gluon exchange taking into account quark correlations in the nucleon, and c) quark exchange.

The hadrons were detected in CLAS [12], a spectrometer with nearly 4π coverage that is based on a toroidal magnetic field ($\sim 1T$) generated by six superconducting coils. The field was set to bend the positive particles away from the beam into the acceptance of the detector. Three drift chamber regions allowed tracking of charged particles [13] and time-of-flight scintillators (TOF) were used for hadron identification [14]. The momentum resolution was of the order of a few percent, while the detector geometric acceptance was about 70% for protons and positive pions. Low energy negative particles, however, were mainly lost at forward angles because they were bent out of the acceptance. Coincidences between the photon tagger and the CLAS detector (TOFs) triggered the recording of hadronic interactions. From a total of 70M triggers, 0.8M events were identified as $p\pi^+\pi^-$ candidates.

The five-fold differential cross section

$$\frac{d\sigma}{d\tau} \equiv \frac{d\sigma(\gamma p \to p\pi^+\pi^-)}{dM_{\pi^+\pi^-}dM_{p\pi^+}d\phi_\rho^{cm}d\phi_{\pi^+}^{decay}dt} \qquad (1)$$

was measured by analyzing all possible event topologies of the reaction $\gamma p \to p\pi^+\pi^-$ with at least two detected hadrons in the final state ($p\pi^+$, $p\pi^-$, $\pi^+\pi^-$, $p\pi^+\pi^-$), using the missing mass and missing energy techniques to eliminate the underlying multi-pion background.

The CLAS acceptance and reconstruction efficiency were evaluated with Monte Carlo simulations. An event generator [15] was used that contained the three main contributions to the $p\pi^+\pi^-$ final state ($\gamma p \to p\rho^0$, $\gamma p \to \Delta^{++}\pi^-$, and $\gamma p \to p\pi^+\pi^-$ in s-wave), along with background reactions with three or more pions. The generated events were processed by a GEANT-based code simulating the CLAS detector that reconstructed the simulated data using the same analysis procedure applied to the raw data. To minimize the model dependence, the acceptance was derived as a function of six independent kinematic variables describing the full three-body reaction, namely, E_γ, the two invariant masses $M_{p\pi^+}$ and $M_{\pi^+\pi^-}$, the ρ^0 center-of-mass azimuthal angle ϕ_ρ^{cm}, the π^+ azimuthal angle in the ρ^0 helicity frame $\phi_{\pi^+}^{decay}$, and the momentum transfer t. For each detected topology, the data were binned in the six dimensional space and corrected, bin by bin, by the corresponding acceptance. Depending on the kinematics, the average acceptance of CLAS for these final states ranges from 5% to 15%.

Each topology predominantly covers complementary kinematic regions. Combining all event topologies together, we were able to measure almost the entire allowed phase space. For $-t < 0.1$ GeV^2 the CLAS detector had no acceptance for the reaction. When multiple topologies were present in the same kinematic region, we considered each topology as an independent measurement of the two pion cross section. Their comparison gave an evaluation of the systematic uncertainty on the cross section ranging from 5% to 10%, depending on the kinematics.

To determine the relative weight of different channels that contribute to the $p\pi^+\pi^-$ final state, the two differential cross sections $d^2\sigma/dtdM_{\pi^+\pi^-}$ and $d^2\sigma/dtdM_{p\pi^+}$ were simultaneously fit to a phenomenological model [16–18] that describes two-pion production as a superposition of three-body phase space and quasi-two-body channels ($\gamma p \to p\rho^0$, $\gamma p \to pf_2(1270)$, $\gamma p \to \Delta^{++}\pi^-$, $\gamma p \to \Delta^0\pi^+$) with subsequent decays. This model describes the cross section as the sum of six amplitudes:

$$\frac{d\sigma}{d\tau} = \left| \sum_{i=1}^{6} a_i T_i \right|^2 . \qquad (2)$$

The complex reaction amplitudes T_i correspond to: 1) diffractive processes in the $\gamma p \to p\rho^0$ reaction (Pomeron and $f_2(1270)$ Regge trajectory exchanges); 2) u-channel exchange in $\gamma p \to p\rho^0$ (nucleon trajectory); 3) Born terms in the $\gamma p \to \Delta^{++}\pi^-$ and $\gamma p \to \Delta^0\pi^+$ reactions (contact and π-in-flight) treated in a Regge approach [19]; 4) ρ^0 Regge trajectory exchange in the reaction $\gamma p \to pf_2(1270)$; 5) s-channel resonance excitation for $p\rho^0$, $\Delta^{++}\pi^-$, and $\Delta^0\pi^+$ (20 well-established resonances were included in the model even though the main contributions come from the $F_{35}(1905)$, $F_{37}(1950)$, and the $G_{17}(2190)$); 6) a phase space parameterized as a real constant number in each (W, t) bin. The ρ^0 and Δ^{++} decay amplitudes were evaluated using an effective Lagrangian model with the form factors as given in Ref. [20].

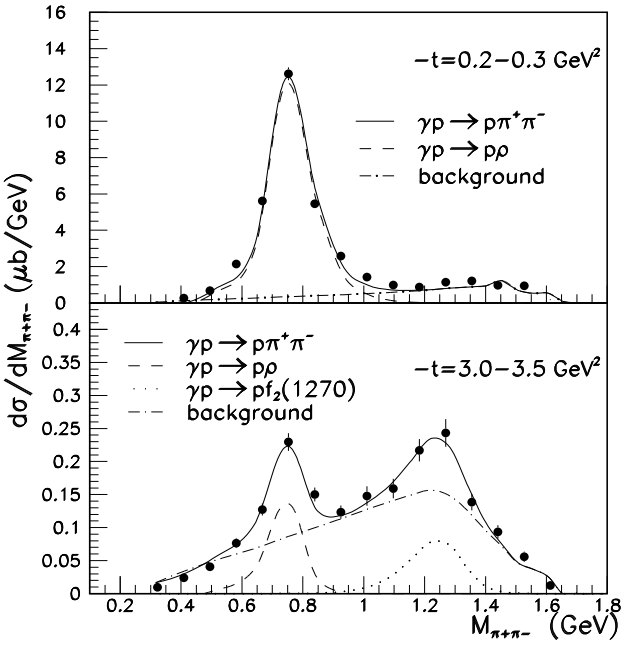

FIG. 2. The measured invariant mass distribution, $M_{\pi^+\pi^-}$, and the fitted quasi-two-body contributions in two t bins: $0.2 - 0.3$ GeV^2 and $3.0 - 3.5$ GeV^2. The solid line corresponds to the coherent sum of different channels.

Figure 2 shows typical invariant mass distributions in a low and a high t bin, and the fitted decomposition into the two-body channels. The real fit parameters a_i, determined in each t bin using MINUIT [21], show a smooth and small dependence on t, indicating that this model can provide a reasonable description of the data.

To evaluate the model dependence, the ρ channel separation was also performed by means of a procedure similar to that used in the ZEUS data analysis [22], fitting the $M_{\pi^+\pi^-}$ distribution with a third-order polynomial background plus Breit-Wigner-shaped lines and an interference term. The extracted ρ^0 cross section agrees within 10% to 30% with the results obtained using the phenomenological model. A full description of the data analysis can be found in Ref. [23].

The extracted ρ^0 photoproduction cross section as a function of t is presented in Fig. 3 for $E_\gamma = 3.8$ GeV. In the low momentum transfer region good agreement with the previous measurement of Ref. [1] is evident.

Assuming an exponential Ae^{Bt} behavior in the range $0.1 < -t < 0.5$ GeV^2, the coefficient resulting from this experiment, $B = -6.4 \pm 0.3$ GeV^{-2}, is consistent with the value $B = -6.9 \pm 0.4$ GeV^{-2} quoted in Ref. [1]. The existing data at large momentum transfer were taken at SLAC [24] with a bremsstrahlung photon beam and a single arm spectrometer; the signal was unfolded from the background using a Breit-Wigner fit but the incomplete detection of the final state did not allow separation of the ω channel from the ρ^0 channel, the latter comprising 50-75% of the data set.

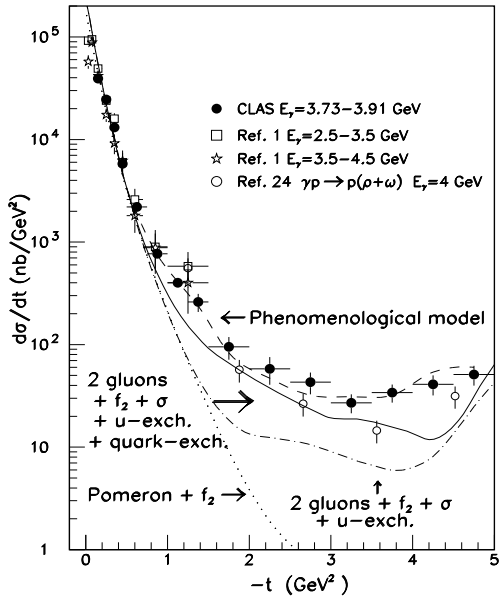

FIG. 3. The differential ρ^0 photoproduction cross section (see text for detailed explanation of the curves). The error bars include statistical and systematic uncertainties summed in quadrature.

Predictions from presently available models are also shown in Fig. 3. The dashed line corresponds to the phenomenological model used for the channel separation assuming that the parameters a_i of equation (2) are independent of t. In this model, the Pomeron and $f_2(1270)$ Regge trajectory exchanges (dotted line) describe the low momentum transfer region, while the large $-t$ flat behavior is reproduced by the tails of resonances having a sizeable branch in the ρ channel. The overall resonance coupling was found to be compatible with what is expected by extrapolating from the low W region by means of a Breit-Wigner shape with an energy-dependent width.

In the QCD-inspired model of Refs. [6,9] (dot-dashed line on Fig. 3), the Pomeron exchange has been replaced by the exchange of two non-perturbatively dressed gluons. At low $-t$ the good agreement with the data is obtained adding the $f_2(1270)$ and the σ Regge trajectories, while the rise at large $-t$ is given by the Reggeized u-channel exchange (N and Δ trajectories) [6]. In this model the gluons can couple to any quark in the ρ meson and in the baryon (see Fig. 1-a,b) and quark correlations in the proton are taken into account assuming the simplest form of its wave function with three valence quarks equally sharing the proton longitudinal momentum [25].

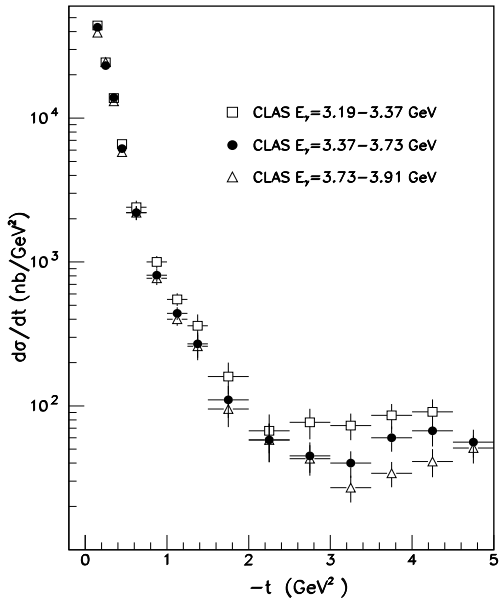

FIG. 4. The energy dependence of the ρ^0 photoproduction $d\sigma/dt$ as measured in CLAS.

The QCD-inspired model describes ϕ photoproduction over the entire t range in our energy region [10], as well as the higher energy ρ^0 SLAC results ($E_\gamma \sim 6$ GeV) [6] where two-gluon exchange is also expected to dominate. Instead, as shown in Fig. 3, the model underestimates the CLAS data, leaving room for quark-exchange processes (Fig. 1-c). As explained in Refs. [19,26,27] these hard-scattering mechanisms can be incorporated in an effective way by using the so called "saturated" trajectory. Regge trajectories are usually linear in t but are expected to "saturate", i.e. be t-independent, at large momentum transfer [28]. The trajectory has been chosen as $\alpha(t) = -1$ when $-t > 3$ GeV^2 [6] to be compatible with quark counting rules [26].

The solid line in Fig. 3 shows the full calculation, including such saturating trajectory. Quark exchange increases the cross section at large $-t$ by a factor two.

Figure 4 shows the measured cross sections in different photon energy bins. From the three data sets, the ρ^0 cross section at $\theta_{cm} = 90°$ is extracted as a function of energy. The power law s^{-C} fit to $d\sigma/dt$ at 90° in the center of mass is performed using both SLAC [2,24] and CLAS data. The fit yields $C = 7.9 \pm 0.3$ ($\chi^2 = 0.6$) showing a good agreement with s^{-8} behavior. The quark exchange diagrams of Fig. 1-c-left (point-like interaction) and 1-c-right (hadronic component of the photon) have a

s^{-7} and s^{-8} power-law behavior respectively, both by dimensional counting [26] and by recent models [29]. Note that also the saturated σ Regge trajectory behaves like s^{-8}. Like the differential cross section at fixed energy, the s dependence suggests the presence of quark interchange hard mechanisms in addition to the two-gluon exchange process.

In conclusion, the full differential two charged-pion cross section was measured for the first time over a large angular range. The differential cross section for $\gamma p \to p\rho^0$ was derived by fitting the $M_{\pi^+\pi^-}$ and $M_{p\pi^+}$ mass distributions with a realistic phenomenological model. The comparison with available models provides indications of the presence of hard processes. Adopting a QCD language in this energy region, the two-gluon exchange mechanisms (that fully describe the ϕ photoproduction data) are not sufficient to reproduce the cross section at large momentum transfer and its energy dependence. Good agreement is achieved when quark interchange processes (suppressed in ϕ production) are included in an effective way in the calculation for the ρ^0 production.

We would like to acknowledge the outstanding efforts of the staff of the Accelerator and the Physics Divisions at JLab that made this experiment possible. This work was supported in part by the Italian Istituto Nazionale di Fisica Nucleare, the French Centre National de la Recherche Scientifique and Commissariat à l'Energie Atomique, the U.S. Department of Energy and National Science Foundation, and the Korea Science and Engineering Foundation. The Southeastern Universities Research Association (SURA) operates the Thomas Jefferson National Accelerator Facility for the United States Department of Energy under contract DE-AC05-84ER40150.

[1] ABBHHM Collaboration, Phys. Rev. **175**, 1669 (1968).
[2] J. Ballam *et al.*, Phys. Rev. **D5**, 545 (1972).
[3] T.H. Bauer *et al.*, Rev. Mod. Phys. **50**, 261 (1978).
[4] B. Friman and M. Soyeur, Nucl. Phys. **A600**, 477 (1996).
[5] Y. Oh, A.I. Titov, T.-S.H. Lee, Proceedings of the NSTAR2000 Conference edited by V. Burkert, L. Elouadrhiri, J. Kelly, R. Minehart, *World Scientific*, p. 255.
[6] J.M. Laget, Phys. Lett. **489B**, 313 (2000).
[7] A. Donnachie and P.V. Landshoff, Phys. Lett. **B185**, 403 (1987).
[8] J.M. Laget and R. Mendez-Galain, Nucl. Phys. **A581**, 397 (1995).
[9] J.M. Laget, *Physics and Instrumentation with 6–12 GeV Beams*, edited by S. Dytman, H. Fenker, and P. Ross (Jefferson Lab User Production, 1998), p. 57.
[10] E. Anciant *et al.*, Phys. Rev. Lett. **85**, 4682 (2000).
[11] D.I. Sober *et al.*, Nucl. Instr. and Meth. **A440**, 263 (2000).
[12] W. Brooks, Nucl. Phys. **A663-664**, 1077 (2000).
[13] D. Carman *et al.*, Nucl. Instr. and Meth. **A449**, 81 (2000).
[14] E.S. Smith *et al.*, Nucl. Instr. and Meth. **A432**, 265 (1999).
[15] P. Corvisiero *et al.*, Nucl. Instr. and Meth. **A346**, 433 (1994).
[16] V. Mokeev *et al.*, Few Body Syst. Suppl. **11**, 292 (1999).
[17] M. Ripani *et al.*, Phys. of Atom. Nucl. **63**, 1943 (2000).
[18] M. Ripani *et al.*, Nucl. Phys. **A672**, 220 (2000).
[19] M. Guidal, J.M. Laget, and M. Vanderhaeghen, Nucl. Phys. **A627**, 645 (1997).
[20] R.B.Longacre and J.Dolbeu, Nucl. Phys. **B122**, 493 (1977).
[21] F.James CERN Program Library D506.
[22] The ZEUS Collaboration Eur. Phys. J. **C14**, 213 (2000).
[23] M. Battaglieri, CLAS-Analysis 2001-002 May 2001 `http://www.jlab.org/Hall-B/pubs/analysis/battaglieri_rho.ps`
[24] R.L. Anderson *et al.*, Phys. Rev. **D14**, 679 (1976).
[25] J.R. Cudell and B.U. Nguyen, Nucl. Phys. **B420**, 669 (1994).
[26] S.J. Brodsky and G.R. Farrar, Phys. Rev. Lett. **31**, 1153 (1973).
[27] P.D.B Collins and P.J. Kearney, Z. Phys. **C22**, 277 (1984).
[28] M.N. Sergeenko, Z. Phys. **C64**, 315 (1994).
[29] H.W Huang and P. Kroll, Eur. Phys. J. **C17**, 423 (2000).